

REFERENCES

Acquaviva, S. J., Birchon, D., Carlyle, J. M., Faller, J. G., Graham, L. J., Hart, S. D., McBride, S. L., Scott, I. G., Stone, D. E. W. and Vanderveldt, H. H., 1980, "Interlaboratory Comparisons of Acoustic Emission Spectra", **NDT International**, Vol. 13, No. 5, pp. 230-234.

Agilent Technologies, 2000, **89410A/89441A Operator's Guide**, Washington, USA.

Alvarez, M. G., Lapitz, P. and Ruzzante, J., 2008, "AE Response of Type 304 Stainless Steel during Stress Corrosion Crack Propagation", **Corrosion Science**, Vol. 50, No. 12, pp. 3382 - 3388.

Andreykiv, O. Y., Lysak, M. V., Serhiyenko, O. M. and Skalsky, V. R., 2001, "Analysis of Acoustic Emission Caused by Internal Cracks", **Engineering Fracture Mechanics**, Vol. 68, No. 11, pp. 1317-1333.

APC International, 2002, **Piezoelectric Ceramics: Principles and Applications**, Mackeyville, Pennsylvania, USA, pp. 6-33.

Arora, A., 1984, "Acoustic Emission Characterization of Corrosion Reactions in Aluminum Alloys", **CORROSION**, Vol. 40, No. 9, pp. 459 - 465.

Assouli, B., Simescu, F., Debicki, G. and Idrissi, H., 2005, "Detection and Identification of Concrete Cracking during Corrosion of Reinforced Concrete by Acoustic Emission Coupled to the Electrochemical Techniques", **NDT & E International**, Vol. 38, No. 8, pp. 682-689.

ASTM International, 1998, **ASTM E1781: Standard Practice for Secondary Calibration of Acoustic Emission Sensors**, Pennsylvania, USA, pp. 1-7.

ASTM International, 2005, **ASTM E976: Standard Guide for Determining the Reproducibility of Acoustic Emission Sensor Response**, Pennsylvania, USA, pp. 1-7.

ASTM International, 2007, **ASTM E1106: Standard Test Method for Primary Calibration of Acoustic Emission Sensors**, Pennsylvania, USA, pp. 1-11.

ASTM International, 2011, **ASTM E1316: Standard Terminology for Nondestructive Examinations**, Pennsylvania, USA, pp. 3-6.

Bailey, C. D., Hamilton, J. M. and Pless, W. M., 1976, "AE Monitoring of Rapid Crack Growth in a Production-Size Wing Fatigue Test Article", **NDT International**, Vol. 9, No. 6, pp. 298-304.

Barron, R. F., 2003, **Industrial Noise Control and Acoustics**, Marcel Dekker Inc., New York, USA, pp. 97 - 107.

Bellenger, F., Mazille, H. and Idrissi, H., 2002, "Use of Acoustic Emission Technique for the Early Detection of Aluminum Alloys Exfoliation Corrosion", **NDT & E International**, Vol. 35, No. 6, pp. 385-392.

- Bolin, L., 1979, "A model for Estimating the Signal from an Acoustic Emission Source", **Ultrasonics**, Vol. 17, No. 2, pp. 67-70.
- Bowles, S. J., 1989, "AE Load-Cycle Dependence Applied to Monitoring Fatigue Crack Growth under Complex Loading Conditions" **NDT International**, Vol. 22, No. 1, pp. 7-13.
- Breckenridge, F. R., 1982, "Acoustic Emission Transducer Calibration by Means of the Seismic Surface Pulse", **Journal of Acoustic Emission**, Vol. 1, No. 2, pp. 87 - 94.
- Breckenridge, F. R., Proctor, T. M., Hsu, N. N. and Eitzen, D. G., 1984, "Some Notions Concerning the Behaviour of Transducers", **National Bureau of Standards**, Gaithersburg.
- Callens, D., Bruneel, C. and Assaad, J., 2004, "Matching Ultrasonic Transducer using Two Matching Layers Where One of Them is Glue", **NDT & E International**, Vol. 37, No. 8, pp. 591-596.
- Chen, P., Chua, P. S. K. and Lim, G. H., 2005, "An Experimental Study of Monitoring Internal Leakage in Water Hydraulic Cylinders Using Acoustic Emission", **Journal of Testing and Evaluation**, Vol. 33, No. 6, pp. 1-7.
- Chen, P., Chua, P. S. K. and Lim, G. H., 2007, "A Study of Hydraulic Seal Integrity", **Mechanical Systems and Signal Processing**, Vol. 21, No. 2, pp. 1115-1126.
- Clough, R.B., 1987, "Energetics of Acoustic Emission Source Characterization", **Material Evaluation**, Vol. 45, No. 5, pp. 556-563.
- Cunfu, H., Lijun, H. and Bin, W., 2007, "Design of a Piezoelectric Transducer Cylindrical Phase Modulator for Simulating Acoustic Emission Signals", **Frontiers of Mechanical Engineering in China**, Vol. 2, No. 3, pp. 370-373.
- Darowicki, K., Mirakowski, A. and Krakowiak, S., 2003, "Investigation of Pitting Corrosion of Stainless Steel by Means of Acoustic Emission and Potentiodynamic Method", **Corrosion Science**, Vol. 45, No. 8, pp. 1747-1756.
- Don, M., Dennis, M. and Veijo, S., 1999, **Transducer Backing Material and Method of Application**, US. International Patent, No. WO 99/57939.
- Dunegan, H. L., 2003, "Considerations for Selection of Advanced AE Transducer", **DECI Report: May 2003**.
- Dunn, S. E., Young, J. D., Hartt, W. H. and Brown, R. P., 1984, "Acoustic Emission Characterization of Corrosion Induced Damage in Reinforced Concrete", **CORROSION**, Vol.40, No. 7, pp. 339-343.
- Evans, M. J., 1997, **The Use of Diffuse Field Measurements for Acoustic Emission**, Thesis of Doctor of Philosophy, Department of Mechanical Engineering, Imperial College of Science, Technology and Medicine, University of London.

- Evans, M. J., Webster, J. R. and Cawley, P., 2000, "Design of a Self-Calibration Simulated Acoustic Emission Source", **Ultrasonics**, Vol. 37, No. 8, pp. 589-594.
- Ferrer, F., Faure, T., Goudiakas, J. and Andres, E., 2002, "Acoustic Emission Study of Active-Passive Transitions During Carbon Steel Erosion-Corrosion in Concentrated Sulfuric Acid", **Corrosion Science**, Vol. 44, No. 7, pp. 1529-1540.
- Ferrer, F., Idrissi, H., Mazille, H., Fleischmann, P. And Labeeuw, P., 1999, "On the Potential of Acoustic Emission for the Characterization and Understanding of Mechanical Damaging During Abrasion-Corrosion Processes", **Wear**, Vol. 231, No. 1, pp. 108-115.
- Ferrer, F., Idrissi, H., Mazille, H., Fleischmann, P. And Labeeuw, P., 2000, "A Study of Abrasion-Corrosion of AISI 304L Austenitic Stainless Steel in Saline Solution using Acoustic Emission Technique", **NDT & E International**, Vol. 33, No. 6, pp. 383-371.
- Flitt, H. J. and Schweinsberg, D. P., 2010, "Synthesis, Matching and Deconstruction of Polarization Curves for the Active Corrosion of Zinc in Aerated Near-Neutral NaCl Solutions", **Corrosion Science**, Vol. 52, No. 6, pp. 1905 - 1914.
- Fortunko, C. M., Hamstad, M. A. and Fitting, D. W., 1992, "High-Fidelity Acoustic-Emission Sensor/Preamplifier Subsystems: Modeling and Experiments", **Ultrasonics Symposium 1992**, October 20-23, Arizona, USA, pp.327-332.
- Green, G.A., 1978, "A Simple Method for the Direct Comparison of Acoustic Emission Detection Systems", **NDT International**, Vol. 11, No. 2, pp. 69-71.
- Hanato. H, 1975, "Quantitative Measurements of Acoustic Emission Related to Its Microscopic Mechanisms", **Journal of Acoustic Emission**, Vol. 57, No. 3, pp. 639-645.
- Hill, R. and El-dardiry, S. M. A., 1981, "Variables in the Use and Design of Acoustic Emission Transducers", **Ultrasonics**, Vol. 19, No. 1, pp. 9-16.
- Hill, R., Cowking, A., and Carswell, W. S., 1989, "An Acoustic Emission Study of Stress Corrosion in a Chopped Strand Mat GFRP Composite", **COMPOSITES**, Vol. 20, No. 3, pp. 215-222.
- Holroyd, T. J. and Matlock, N., 1995, **Resonant Acoustic Emission Transducer**, US. Patent, No. 5,452,264.
- Hong, J., Yoo, J., Lee, K., Lee, S. and Song, H., 2008, "Characteristics of Acoustic Emission Sensor Using Lead-Free (LiNaK)(NaTaSb)O₃ Ceramics for Fluid Leak Detection at Power Plant Valves", **Japanese Journal of Applied Physics**, Vol. 47, No. 4, pp. 2192-2194.
- Ing, M., Austin, S. and Lyons, R., 2005, "Cover Zone Properties Influencing Acoustic Emission due to Corrosion", **Cement and Concrete Research**, Vol. 35, No. 2, pp.284-295.



- Jirarungsatian, C. and Prateepasen, A., 2010, "Pitting and Uniform Corrosion Source Recognition using Acoustic Emission Parameters", **Corrosion Science**, Vol. 52, No. 1, pp. 187-197.
- Jirarungsatian, C., Prateepasen, A. and Kaewtrakulpong, 2005, "Monitoring of Pitting Corrosion in Stainless Steels using Acoustic Emission", **Journal of Non-Destructive Testing-Australia**, Vol. 42, No. 3, pp. 76-81.
- Jomdecha, C., Prateepasen, A., Kaewtrakulpong, P., and Thungsuk, P., 2004, "Corrosion-Source Location by an FPGA-PC Based Acoustic-Emission System", **IEEE Region 10 Annual International Conference (TENCON)**, Chiangmai, Thailand, pp. D601-D604.
- Jomdecha, C., Prateepasen, A. and Kaewtrakulpong, P., 2007, "A Study on Source Location using an Acoustic Emission System on Various Types", **NDT&E International**, Vol. 40, No. 8, pp. 584-593.
- Jomdecha, C. and Prateepasen, A., 2006, "A Resonance Acoustic Emission Sensor Using Single Piezoelectric Ceramic: Characteristic and Performances", **KMUTT Research and Development Journal**, Vol. 29, No. 4, pp. 483 – 498.
- Jones, B.E. and Yan, T., 2005, "Acoustic Emission Traceable Sensing", **Journal of Strain Analysis**, Vol. 40, No.1, pp.17-23.
- Jones, D. A., 1997, **Principles and Prevention of Corrosion**, Simon & Schuster (Asia) Pte, Ltd., Singapore, p.75.
- Jones, R. H. and Friesel, M. A., 1992, "Acoustic Emission During Pitting and Transgranular Crack Initiation in Type 304 Stainless Steel", **CORROSION**, Vol. 48, No. 9, pp.751-758.
- Jones, R. H., Friesel, M. A. and Pathania, R., 1991, "Evaluation of Stress Corrosion Crack Initiation Using Acoustic Emission", **CORROSION**, Vol. 47, No. 2, pp.105-115.
- Kaewwaewnoi, W., Prateepasen, A., and Kaewtrakulpong, P., 2005, "Measurement of Valve Leakage Rate using Acoustic Emission", **The 2005 Electrical Engineering/Electronics, Computer, Telecommunications, and Information Technology International Conference (ECTI-CON 2005)**, May 12-13, Cholburi, Thailand, pp. 597-600.
- Kaewwaewnoi, W., Prateepasen, A. and Kaewtrakulpong, P., 2007, "A Study on Correlation of AE Signals from Different AE Sensors in Valve Leakage Rate Detection", **ECTI TRANSACTIONS ON ELECTRICAL ENG., ELECTRONICS, AND COMMUNICATIONS**, Vol. 5, No. 1, pp. 113-117.
- Kaewwaewnoi, W., Prateepasen, A. and Kaewtrakulpong, P., 2010, "Investigation of the Relationship between Internal Fluid Leakage through a Valve and the Acoustic Emission Generated from the Leakage", **Measurement**, Vol. 43, No. 2, pp. 274-282.

- Kasai, N., Utatsu, K., Park, S., Kitsukawa, S., and Sekine, K., 2009, "Correlation between Corrosion Rate and AE Signal in an Acidic Environment for Mild Steel", **Corrosion Science**, Vol. 51, No. 8, pp. 1679-1684.
- Kazys, R., Voleisis, A. and Voleisiene, B., 2008, "High Temperature Ultrasonic Transducers: Review", **ULTRAGARSAS (ULTRASOUND)**, Vol. 63, No.2, pp. 7-17.
- Keprt, J. and Benes, P., 2007, "Determination of Uncertainty in Calibration of Acoustic Emission Sensors", **4th International Conference on NDT**, October 11-14, Chania, Crete-Greece, pp. 1-8.
- Keprt, J. and Benes, P., 2008, "A Comparison of AE Sensor Calibration Methods", **Journal of Acoustic Emission**, Vol. 26, pp. 60 - 71.
- Keprt, J. and Benes, P., 2008, "Progress in Primary Calibration of Acoustic Emission Sensors", **Acoustics'08 Paris Press Conferences**, June 29 – July 4, Paris, France, pp. 2217-2222.
- Kino, G. S., 1987, **Acoustic Waves: Devices, Imaging, and Analog Signal Processing**, Prentice-Hall, Inc., New Jersey, USA, pp. 94-101.
- Kirk, K. J., Scheit, C. W. and Schmarje, N., 2007, "High-Temperature Acoustic Emission Tests using Lithium Niobate Piezocomposite Transducers", **Insight**, Vol. 49, No. 3, pp. 142-145.
- Kudryavtsev, V. N., Schmitt-Thomas, Kh, G., Stengle, W. And Waterschek, R., 1981, "Detection of Hydrogen Embrittlement of a Carbon Steel by Acoustic Emission", **CORROSION**, Vol. 37, No. 12, pp. 690-695.
- Lee, J. H., Lee, M. R., Kim, J. T., Kim, J. S. and Luk, V. K., 2003, "Condition Monitoring of a Check Valve for Nuclear Power Plants by Means of Acoustic Emission Technique", **Transactions of the 17th International Conference on Structural Mechanics in Reactor Technology (SMiRT 17)**, August 17-22, Prague, Czech Republic, pp. 1-8.
- Lee, J. H., Lee, M. R., Kim, J. T. and Kim, J. S., 2004, "Analysis of Acoustic Emission Signals for Condition Monitoring of Check Valve at Nuclear Power Plants", **Key Engineering Materials**, Vol. 270-273, pp. 531-536.
- Lee, M. R., Lee, J. H. and Kim, J. T., 2005, "Condition Monitoring of a Nuclear Power Plant Check Valve Based on Acoustic Emission and a Neural Network", **Journal of Pressure Vessel Technology**, Vol. 127, No. 3, pp. 230-236.
- Lee, J. H., Lee, M. R., Kim, J. T., Luk, V. and Jung, Y. H., 2006, "A Study of the Characteristics of the Acoustic Emission Signals for Condition Monitoring of Check Valves in Nuclear Power Plants", **Nuclear Engineering and Design**, Vol. 236, No. 13, pp. 1411-1421.

Lee, S. G., Park, J. H., Yoo, K. B., Lee, S. K. and Hong, S. Y., 2006, "Evaluation of Internal Leak in Valve Using Acoustic Emission Method", **Key Engineering Materials**, Vol. 326-328, pp. 661-664.

Lee, Y. L. and Lin, Z., 2006, "Miniature Piezoelectric Conical Transducer: Fabrication, Evaluation and Application", **Ultrasonics**, Vol. 44, No. 1 (Supplement 1), pp. 693-697.

LOCAN 320 User's manual, 1990, Physical Acoustics Corporation, Princeton, New Jersey, USA.

Mansfeld, F., 2005, "Tafel Slopes and Corrosion Rates Obtained in the Pre-Tafel Region of Polarization Curves", **Corrosion Science**, Vol. 47, No. 12, pp. 3178-3186.

McIntire, P., 1987, **Nondestructive Testing Handbook Second Edition: Volume 5 Acoustic Emission Testing**, American Society for Nondestructive Testing, Columbus, OH, USA, pp. 27 - 29, 97 - 107, 122- 132.

Merhaut, J., 1981, **Theory of Electroacoustics**, 1st edition, McGraw-Hill, USA, pp. 2-5, 75-78, 231-237, 274-281.

Noipitak, M., Laoratanakul, P. and Prateepasen, A., 2007, "Design and Development of Ultrasonic Probe for Residual Stress Measurement", **IE Network Conference 2007**, October 24 - 26, Phuket, Thailand, pp. 1397 - 1402.

Ohtsu, M. and Ono, K., 1988, "AE Source Location and Orientation Determination of Tensile Cracks from Surface Observation", **NDT International**, Vol. 21, No. 3, pp. 143- 150.

Pollock, A.A. and Hsu, S.Y.S., 1982, "Leak Detection using Acoustic Emission", **Journal of Acoustic Emission**, Vol. 1, No. 4, pp. 237-243.

Prateepasen, A., Au, Y. H. J. And Jones, B. E., 2000, "Calibration of Acoustic Emission for Tool Wear Monitoring", **XVI IMEKO World Congress**, September 25-28, Vienna, Austria, pp. 255-260.

Prateepasen, A., Au, Y. H. J. And Jones, B. E., 2000, "Comparison of Artificial Acoustic Emission Sources as Calibration Sources for Tool Wear Monitoring in Single-Point Machining", **Journal of Acoustic Emission**, Vol. 18, pp. 196-204.

Prateepasen, A., Jirarungsatean, C., and Tuengsook, P., 2006, "Identification of AE Source in Corrosion Process", **Key Engineering Materials**, Vol. 321-323, pp. 545-548.

Prateepasen, A., Jirarungsatean, C., and Tuengsook, P., 2006, "Effect of Sulfuric Acid Concentration on Acoustic Emission Signals in Uniform-Corrosion", **Key Engineering Materials**, Vol. 321-323, pp. 553-556.

Prateepasen, A. and Srinang, M., 2008, "Acoustic Emission Transferability using Transfer Function", **17th World Conference on Nondestructive Testing**, October 25-28, Shanghai, China, pp. 1-8.

- Raeymaekers, B. and Talke, F. E., 2006, "The use of Acoustic Emission for Detection of Tape Edge Contact", **ASME/JSME Joint Conference on Micromechatronics for Information and Precision Equipment (MIPE 2006)**, June 21-23, California, United States of America, pp. 1-3.
- Ramadan, S., Gaillet, L., Tessier, C. and Idrissi, H., 2008, "Detection of Stress Corrosion Cracking of High-Strength Steel used in Prestressed Concrete Structure by Acoustic Emission Technique", **Applied Surface Science**, Vol. 254, No. 8, pp. 2255-2261.
- Saenkhum, N., Prateepasen, A., and Keawtrakulpong, P., 2003, "Classification of Corrosion Detected by Acoustic Emission", **2003 ASME International Mechanical Engineering Congress & Exposition**, November 15-21, Washington, United States of America, pp. 1-9.
- Seah, K. H. W., Lim, K. B., Chew, C. H. and Teoh, S. H., 1993, "The Correlation of Acoustic Emission with Rate of Corrosion", **Corrosion Science**, Vol. 34, No. 10, pp. 1707-1713.
- Shaikh, H., Amirthalingam, R., Anita, T., Sivaibharasi, N., Jaykumar, T., Manohar, P. and Khatak, H. S., 2007, "Evaluation of Stress Corrosion Cracking Phenomenon in an AISI Type 316LN Stainless Steel Using Acoustic Emission Technique", **Corrosion Science**, Vol. 49, No. 2, pp. 740-765.
- Sharif, M. A. and Grosvenor, R. I., 1998, "Internal Valve Leakage Detection Using an Acoustic Emission Measurement System", **Transactions of the Institute of Measurement and Control**, Vol. 20, NO. 5, pp. 233-242.
- Sherrit, S., Leary, S. P., Dolgin, B. P. and Bar-Cohen, Y., 1999, "Comparison of the Mason and KLM Equivalent Circuits for Piezoelectric Resonators in the Thickness Mode", **Ultrasonics Symposium**, Vol. 2, pp. 921-926.
- State, M., Brands, P. J. and Vosse, F. N., 2010, "Improving the Thermal Dimensional Stability of Flexible Polymer Composite Backing Materials for Ultrasound Transducers", **Ultrasonics**, Vol. 50, No. 4, pp. 458-466.
- Sugishita, T. and Ku, M., 1997, **Piezoelectric Transducer**, US. Patent, No. 5,828,160.
- Tantawy, F. D. and Sung, Y. K., 2003, "A Novel Ultrasonic Transducer Backing from Porous Epoxy Resin-Titanium-Silane Coupling Agent and Plasticizer Composites", **Materials Letters**, Vol. 58, No. 1, pp.154-158.
- Theobald, P., 2004, "Towards Traceable Calibration of Acoustic Emission Measurement Systems: Development of a Reference Source at the UK's National Physical Laboratory", **26th European Conference on Acoustic Emission testing (EWGAE 2010)**, September 15-17, Berlin, Germany, pp. 683-690.
- Theobald, P.D., 2009, "Optical Calibration for Both Out-of-plane and In-plane Displacement Sensitivity of Acoustic Emission Sensors", **Ultrasonics**, Vol. 49, pp. 623-627.

Theobald, P. and Pocklington, R., 2010, "Velocity Sensitivity Calibration of AE Sensors using the Through Wave Method and Laser Interferometry", **29th European Conference on Acoustic Emission testing (EWGAE 2010)**, September 8-10, Vienna, Austria, pp. 1-7.

Theobald, P., Esward, T. J., Dowson, S. P. and Preston, R. C., 2005, "Acoustic Emission Transducer—Development of a Facility for Traceable Out-of-Plane Displacement Calibration", **Ultrasonics**, Vol. 43, No. 5, pp. 343-350.

Theobald, P., Rakowski, R. T., Yan, T., Jarvis, D., Dowson, S. and Jones, B. E., 2001, "Reference Source for the Calibration of Acoustic Emission Measurement", **IEEE Instrumentation and Measurement Technology Conference**, May 21-23, Budapest, Hungary, pp. 412-416.

Weng, M. S., Dunn, S. E., Hartt, W. H. and Brown, R. P., 1982, "Application of Acoustic Emission to Detection of Reinforcing Steel Corrosion in Concrete", **CORROSION**, Vol. 38, No. 1, pp. 9-14.

Yan, T. and Jones, B.E., 2000, "Traceability of Acoustic Emission Measurements using Energy Calibration Method", **Measurement Science and Technology**, Vol. 11, pp. 9-12.

Yan, T., Theobald, P., and Jones, B.E., 2002, "A Self-Calibrating Piezoelectric Transducer with Integral Sensor for In Situ Energy Calibration of Acoustic Emission", **NDT & E International**, Vol. 35, No. 7, pp. 459-464.

Yan, T., Theobald, P., and Jones, B.E., 2004, "A Conical Piezoelectric Transducer with Integral Sensor as a Self-calibrating Acoustic Emission Energy Source", **Ultrasonics**, Vol. 42, No. 4, pp. 431-438.

Yarovikov, V.I. and Bazhenov, A.A., 1998, "Analysis of Piezoelectric Ultrasonic Receivers based on the Equations of Electroelasticity when the Sensitive Element is in a State of Bulk Stress", **Measurement Techniques**, Vol. 41, No. 7, pp. 661-666.

Yonezu, A., Cho, H. and Takemoto, M., 2006, "Monitoring of Stress Corrosion Cracking in Stainless Steel Weldments by Acoustic and Electrochemical Measurements", **Measurement Science and Technology**, Vol. 17, No. 9, pp. 2447-2454.

Yuki, H. and Homma, K., 1996, "Estimation of Acoustic Emission Source Waveform of Fracture using a Neural Network", **NDT&E International**, Vol. 29, No. 1, pp. 21-25.

Zhang, W., Dunbar, L. and Tice, D., 2008, "Monitoring of Stress Corrosion Cracking of Sensitized 304H Stainless Steel in Nuclear Applications by Electrochemical Methods and Acoustic Emission", **Energy Materials: Materials Science and Engineering for Energy Systems**, Vol. 3, No. 2, pp. 59-71.

APPENDIX A

Simulation of Aperture Effect Using MATLAB

The aperture effect of home-built AE sensor is calculated for Rayleigh velocity in steel of 3,000 m/sec using MATLAB software. The calculated result is shown below.

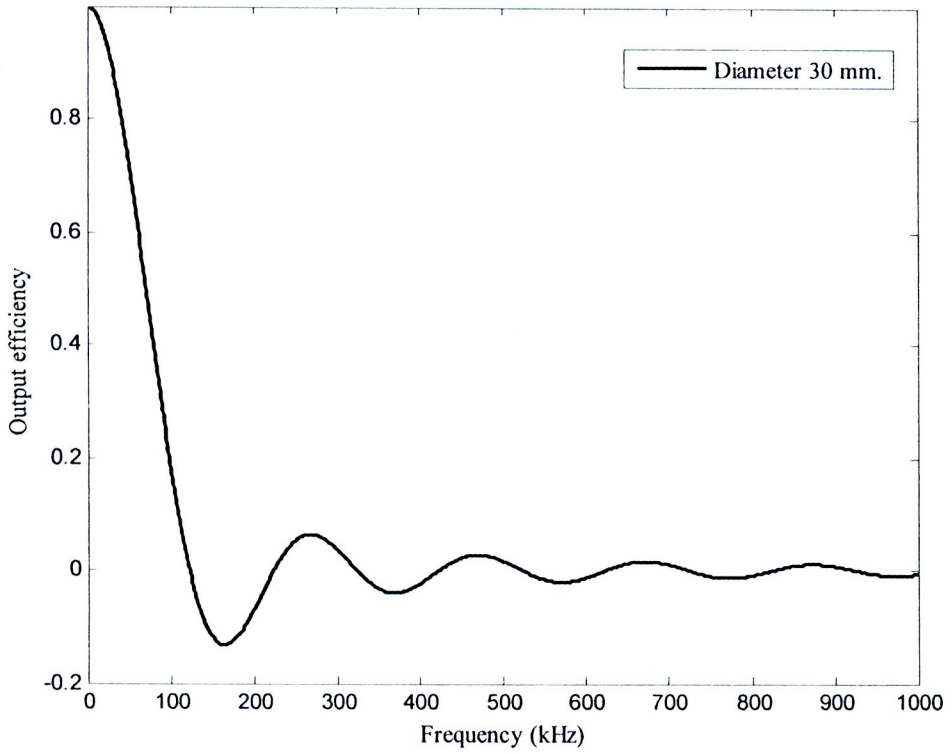


Figure A.1 Simulation of aperture effect using MATLAB

APPENDIX B

Definitions of PZT Material

The some definitions and constants of PZT element according to APC International (2002) are summarized here.

The piezoelectric charge constant (d) is the polarization created per unit of mechanical stress (T) applied to a PZT material or, alternatively, is the mechanical strain (σ) experienced by a PZT material per unit of electric field applied. The first subscript to d is the direction of polarization created in the material when the electric field (E_p) is zero or alternatively is the direction of the applied field strength. The second subscript is the direction of the applied stress or the induced strain, respectively. Because the strain induced in a PZT material by an applied electric field is the product of the value for the electric field and the value for d , d is an important indicator of a suitability of material for strain-dependent applications. The details of piezoelectric charge constant are shown below.

d_{33} is induced polarization in direction 3 (parallel to direction in which ceramic element is polarized) per unit stress applied in direction 3 or induced strain in direction 3 per unit electric field applied in direction 3.

d_{31} is induced polarization in direction 3 (parallel to direction in which ceramic element is polarized) per unit stress applied in direction 1 (perpendicular to direction in which ceramic element is polarized) or induced strain in direction 1 per unit electric field applied in direction 3.

d_{15} is induced polarization in direction 1 (perpendicular to direction in which ceramic element is polarized) per unit shear stress applied about direction 2 (direction 2 perpendicular to direction in which ceramic element is polarized) or induced shear strain about direction 2 per unit electric field applied in direction 1.

The piezoelectric voltage constant (g) is the electric field created by a PZT material per unit of mechanical stress applied or alternatively is the mechanical strain experienced by PZT material per unit of electric displacement applied. The first subscript to g is the direction of the electric field created in the material, or the direction of the applied electric displacement. The second subscript is the direction of the applied stress or the induced strain, respectively. Because the strength of the induced electric field produced by a PZT material in response to an applied physical stress is the product of the value for the applied stress and the value for g , g is important for assessing a suitability of material for sensor applications. The details of piezoelectric voltage constant are shown below.

g_{33} is induced electric field in direction 3 (parallel to direction in which ceramic element is polarized) per unit stress applied in direction 3 or induced strain in direction 3 per unit electric displacement applied in direction 3.

g_{31} is induced electric field in direction 3 (parallel to direction in which ceramic element is polarized) per unit stress applied in direction 1 (perpendicular to direction in which ceramic element is polarized) or induced strain in direction 1 per unit electric displacement applied in direction 3.

g_{15} is induced electric field in direction 1 (perpendicular to direction in which ceramic element is polarized) per unit shear stress applied about direction 2 (direction 2 perpendicular to direction in which ceramic element is polarized) or induced shear strain about direction 2 per unit electric displacement applied in direction 1.

Elastic compliance (s) is the strain produced in a PZT material per unit of stress applied. For the 11 and 33 directions, it is the reciprocal of the modulus of elasticity (Young's modulus, ζ). s^D is the compliance under a constant electric displacement and s^E is the compliance under a constant electric field. The first subscript is the direction of strain. The second is the direction of stress. The details of elastic compliance are shown below.

s_{33}^D is the elastic compliance for stress in direction 3 (parallel to direction in which ceramic element is polarized) and accompanying strain in direction 3, under constant electric displacement (open circuit).

s_{11}^E is the elastic compliance for stress in direction 1 (perpendicular to direction in which ceramic element is polarized) and accompanying strain in direction 1, under constant electric field (short circuit).

Young's modulus (ζ) is the stiffness of PZT material. ζ is calculated from the value for the stress applied to the material divided by the value for the resulting strain in the same direction.

The electromechanical coupling factor (k) is an indicator of the effectiveness with that a PZT material converts mechanical energy into electrical energy, or converts electrical energy into mechanical energy. The first subscript to k is the direction along that the electrodes are applied, and the second is the direction along that the mechanical energy is applied.

The values of k quoted in ceramic specifications of manufacturer characteristically are theoretical maximum values. At low input frequency, a typical PZT ceramic can convert 30 - 75% of the energy delivered to it in one form into the other form. It depends on the formulation of the ceramic and the directions of the forces involved. A high value of k usually is desirable for efficient energy conversion, but k is not in itself a measure of efficiency as it does not account for dielectric losses or mechanical losses. Additional, unconverted energy often can be recovery. The accurate measure of efficiency is the ratio of converted, useable energy delivered by the PZT element to the total energy taken up by the element. By this measurement, PZT elements in well designed systems can show efficiencies that exceed 90%.

The dimensions of the PZT element can dictate unique expressions of k . For a thin disc of PZT element the planar coupling factor (k_p) expresses radial coupling, the coupling between an electric field parallel to the direction in which the PZT element is polarized (direction 3) and mechanical effects that produce radial vibrations, relative to the direction of polarization (direction 1 and direction 2). For a disc or plate, the thickness coupling factor (k_t) a unique expression of k_{33} , expresses the coupling between an

electric field in direction 3 and mechanical vibrations in the same direction. The details of each electromechanical coupling factor are shown below.

k_{33} is the factor for electric field in direction 3 for ceramic rod, length $>10 \times$ diameter (parallel to direction in which ceramic element is polarized) and longitudinal vibrations in direction 3.

k_t is the factor for electric field in direction 3 and vibrations in direction 3 for thin disc (surface dimensions large relative to thickness; $k_t < k_{33}$).

k_{31} is the factor for electric field in direction 3 for ceramic rod (parallel to direction in which ceramic element is polarized) and longitudinal vibrations in direction 1 (perpendicular to direction in which ceramic element is polarized).

The dielectric dissipation factor (dielectric loss factor), ($\tan \delta$), is the tangent of the dielectric loss angle. $\tan \delta$ is determined by the ratio of effective conductance to effective susceptibility in a parallel electrical circuit, measured by an impedance bridge. Values for $\tan \delta$ characteristically are determined at 1 kHz.

APPENDIX C

**Analogies between Electrical and Mechanical Systems and Wave Equation for
Thickness Oscillations**

C.1 Analogies between Electrical and Mechanical Systems

In this sub section, the derivation of analogies between electrical and mechanical systems is explained. The details are shown as follows.

From the Newton's second law of motion, the equation is

$$F = \frac{d(mv)}{dt} \quad (C.1)$$

Equation C.1 can be also written as

$$F = m \frac{dv}{dt} \quad (C.2)$$



Since the velocity is small compared with the velocity of light and thus the mass is a constant. In the case of a rectilinear motion, equation C.2 can be written as

$$F = m \frac{d^2 y}{dt^2} \quad (C.3)$$

where y is the displacement from the equilibrium position, and the relation between the velocity and the displacement is

$$v = \frac{dy}{dt} \quad (C.4)$$

The quantities F, v and y in equations C.1 to C.4 can be alternating depend on time. Usually, the harmonic vibrations are interested. In this case, these quantities are sinusoidally dependent on time. Introducing the complex-number notation can be written as

$$y = y_m e^{j\omega t} \quad (C.5)$$

where $\omega = 2\pi f$ is the angular frequency, f is the frequency, and $j = \sqrt{-1}$.

From equations C.4 and C.5 can obtain

$$v = \frac{dy}{dt} = j\omega y_m e^{j\omega t} = v_m e^{j\omega t} = j\omega y \quad (C.6)$$

Similarly, the acceleration

$$\frac{dv}{dt} = j\omega v_m e^{j\omega t} = j\omega v \quad (C.7)$$

From equations C.2 and C.7 can be written as

$$F = j\omega mv \quad (C.8)$$

In an elastic system without mass and friction, the force is proportional to the displacement within the limits of Hooke's law. Thus

$$F = sy = \frac{y}{c_s} \quad (C.9)$$

where s is the stiffness and c_s is the compliance of the system. A relation can be given by

$$s = \frac{1}{c_s}$$

The stiffness can be defined as the force per unit displacement and the compliance can be expressed as displacement per unit force.

Substituting

$$y = \frac{v}{j\omega}$$

putting equation C.6 into C.9 can be written as

$$F = \frac{v}{j\omega c_s} \quad (C.10)$$



The retardation force due to effects of friction in a system during motion is usually proportional to the velocity. The proportionality constant, r_m is called the mechanical resistance. The relationship

$$F = r_m v \quad (C.11)$$

gives the retardation force caused by friction and other losses.

Equations C.8, C.10 and C.11 are reminiscent of the well-known relations between the voltage, u and the current, i in linear electrical circuit theory:

$$u = j\omega Li \quad (C.12)$$

$$u = \frac{i}{j\omega C} \quad (C.13)$$

$$u = Ri \quad (C.14)$$

where L is inductance, C is capacitance, and R is electric resistance.

The analogy between the mechanical and the electrical systems is explained with the force (F) playing the same role as the voltage (u), and the velocity (v) playing the same role as the current (i). The mass (m) in this analogy, has a similar significance in mechanical systems as inductance (L) has in electrical circuits; the mechanical resistance (r) corresponds to the electrical resistance (R); and the compliance (c) has the same significance in mechanical systems as capacitance (C) has in electrical circuits. In this analogy, the displacement (y) of a mechanical system corresponds to electric charge (q), as

$$v = \frac{dy}{dt}$$

so that

$$y = \int v dt$$

and this is analogous to the relationship

$$q = \int i dt$$

between electric charge and current.

In agreement with this is the equation (according to equation C.9)

$$Fc = y$$

which is analogous to the relationship

$$uC = q$$

between the corresponding electrical quantities.

Similarly, as electrical impedance, Z_e is introduced in the theory of electrical circuits as the ratio of voltage to current

$$Z_e = \frac{u}{i}$$

so an analogous quantity, the mechanical impedance, Z_m is introduced there for mechanical systems. It is defined as the ratio

$$Z_m = \frac{F}{v} \tag{C.15}$$

of the force acting on the system to the velocity with which, under the influence of the exciting force, the system vibrates.

The mechanical impedance of a mass is

$$Z_m = j\omega m$$

the mechanical impedance due to friction is equal to the mechanical resistance.

$$Z_m = r$$

And the mechanical impedance associated with elasticity is

$$Z_m = \frac{1}{j\omega c}$$

Equations C.8, C.10 and C.11 can be considered to be the mechanical analogy of Ohm's law, which is a well-known relation in electrical circuit theory.

It is given by the formula

$$v = \frac{F}{Z_m} \quad (\text{C.16})$$

According to this formula the mechanical velocity is proportional to the force and indirectly proportional to the mechanical impedance. In a mechanical system the power is given by

$$P = \frac{1}{T} \int_0^T Fv dt$$

This expression gives a formula analogous to that in electrical circuit theory,

$$P = F_{ef} v_{ef} \cos \varphi \quad (\text{C.17})$$

The relationship between equations C.16 and C.17 are generally valid for any linear mechanical system, that is, for any system where there is a linear dependence between the velocity and the force.

C.2 Wave Equation for Thickness Oscillations

In this sub section, the derivation of wave equation for thickness oscillations is explained.

From the forces acting in the sections x , the increment of force along the length dx is

$$ST_1(x) - ST_1(x + dx) = -S \frac{\partial T_1}{\partial x} dx \quad (\text{C.18})$$

This force (if there is no external force acting in section x) is in equilibrium with the inertial force, which according to Newton's second law is given as a product of the

mass $\rho S dx$ and its acceleration $\partial^2 \eta / \partial t^2$. Therefore, for the equilibrium of forces acting on the element dx , the equation can be written as

$$-\frac{\partial T_1}{\partial x} S dx + \rho \frac{\partial^2 \eta_x}{\partial t^2} S dx = 0 \quad (\text{C.19})$$

and

$$T_1 = \varsigma_{11} \frac{\partial \eta_x}{\partial x} \quad (\text{C.20})$$

This expression can be substituted in equation C.19, which gives after rearrangement

$$\frac{\partial^2 \eta_x}{\partial x^2} = \frac{\rho}{\varsigma_{11}} \frac{\partial^2 \eta_x}{\partial t^2} \quad (\text{C.21})$$

Equation C.21 is the wave equation of oscillations propagating in the x direction. Its general form is

$$\frac{\partial^2 \eta_x}{\partial x^2} = \frac{1}{c_0^2} \frac{\partial^2 \eta_x}{\partial t^2} \quad (\text{C.22})$$

where c_0 is the velocity of propagation of mechanical oscillations in the x direction. Comparing equations C.21 and C.22

$$c_0 = \sqrt{\frac{\varsigma_{11}}{\rho}} \quad (\text{C.23})$$

Considering only harmonic oscillations of frequency f , the equation can be written as

$$\eta_x = \eta_{xm} e^{j\omega t} \quad (\text{C.24})$$

where $\omega = 2\pi f$. Then

$$\frac{\partial^2 \eta_x}{\partial t^2} = -\omega^2 \eta_x \quad (\text{C.25})$$

Substituting equation C.25 into C.22, for the time-independent part of η_x , the equation can be written as

$$\frac{\partial^2 \eta_x}{\partial x^2} + k^2 \eta_x = 0 \quad (\text{C.26})$$

where $k = \omega / c_0$ is the wave number.

APPENDIX D

Characteristic of Tungsten Powder (Backing Material)

Table D.1 Characteristic of tungsten powder

1568754 DMTMP200 TUNGSTEN TMP200 300C F7098				
Characteristic	Unit	Value	Lower Upper	
Batch: F03810886 / Quantity 10,000 kg				
TOTAL CARBON	%	0.02	SPEC: 0.00 – 0.15	
OXYGEN	%	0.10	SPEC: 0.00 – 0.15	
IRON	%	0.1	SPEC: 0.0 – 0.2	
APP DENS	g / cm ³	9	SPEC: 7 – 10	
APP DENS	GI3	154.4	MIN: 0.0	
TAP DENSITY	g / cm ³	11.6	SPEC: 10.0 – 13.0	
TAP DENSITY	GI3	190.6	MIN: 0.0	
HALL FLOW	S	7	UPPER SPEC: 10	
+ 100	%	0.3	MAX: 1.0	
+ 100 + 140	%	10.2	SPEC: 5.0 – 20.0	
+ 140 + 200	%	22.2	SPEC: 15.0 – 30.0	
+ 200 + 325	%	41.9	SPEC: 30.0 – 50.0	
+ 325 + 400	%	15.4	SPEC: 5.0 – 20.0	
+ 400	%	10.0	MAX: 15.0	

APPENDIX E

LOCAN 320 Setting

E.1 Introduction of LOCAN 320

A LOCAN 320 AE acquisition from Physical Acoustics Corporation (PAC) was used in this study. The LOCAN 320 is a computerized AE system that performs AE signal measurements, stores, displays and analyzes the resulting data in real time. The AE signal from the AE sources (leakage and corrosion) are converted into electrical signals by the AE sensor, amplified to useable voltage levels by the preamplifiers and measured in two-channel computerized modules known as Independent Channel Controllers (ICCs). Each source event may be detected by one, two or eight channels. The important components of internal and external hardware show follow.

Processor:	80286 20MHz
Co-processor:	80C287
BIOS:	100% IBM PC/AT compatible
Operating System:	MS-DOS, (Version 3.3)
RAM:	2 MByte
Storage:	40 MByte Hard Disk
Power Supply:	200 Watt Digital 100 Watt Analog
Slots/Channels:	Eight (8)

AE Signal Measurements (Based on ICC Analog)

Bandwidth:	3 kHz to 1 MHz
Noise:	18 dB (with 40 dB gain setting)
Gain Setting:	0 to 60 dB in 1 dB steps
Gain Accuracy:	+/- 1 dB
Threshold (fixed):	20 mV to 2.5 V range 10 mV resolution 3 mV accuracy Auto set by ICC computer in range of 12 to 88 dB
Threshold (floating):	50 mV to 12 V (DC) range

E.2 LOCAN 320 Setting

Turn the power on using the switch located on the rear panel and uses the following sequence to set the AE data acquisition.

- Press Esc and press del, and then select Run Cmos

- Setting Cmos (press Page Up and Page Down)

Hard Disk C: 47 = user type	Cyln	Head	WDcomp	Lzone	Sect	Size
	826	16	825	0	63	-

Hard Disk D: not installed

VDO VGA

Keyboard Installed

For exit, press Esc, enter Y and press Enter

The computer starts the program.

Press Esc and press del, and then select Run Xcmos Set up

- Select ADVANCED NEAT CHIPSET REGISTER SET UP

- Setting Xcmos (press Page up and Page Down)

82 C211

60H	00	0	0	R	0	R0
61H	0	1	00	01	01	
62H	RR		11	11	10	

82 C212B

6AH	11	1	RRRR			
6BH	1	1	0	0	10	11

For exit, press Esc and select WRITE CMOS REGISTERS AND EXIT

Waiting the program:

Enter l320loc on the Dos command, and press Enter

E.3 Hardware Setting

The hardware setting must be selected before the test. The structure of this menu is divided into four blocks: Channel Setting, Hit Data Set, Time Driven Data Set and Parametric Multiplier/Offset. To move the cursor between these blocks, use the TAB key and to move the cursor within each block, use the four arrow keys in the right-hand section of the keyboard.

In this study, the value of parameter in channel setting block was set as shown follow.

GAIN (Main Amplifier)	=	20 dB (valve leakage), 32 dB (corrosion)
PDT (usec)	=	300
HDT (usec)	=	600
HLT (usec)	=	1000
Threshold (dB)	=	Fix 50

Note: Amplified signal by preamplifier = 40 dB (valve leakage), 60 dB (corrosion)

APPENDIX F

HP 89410A Vector Signal Analyzer Setting

A HP 89410A Vector Signal Analyzer was used to determine the characteristic of AE signal in term of frequency response. The Vector Signal Analyzer has a frequency bandwidth of 0 to 10 MHz and frequency points of 51 to 3201 points. In order to optimize the measurement, measurement speed, measurement resolution and display resolution are considered. For determining measurement resolution and measurement speed, resolution bandwidth, frequency span, main length and window selection are also considered (Agilent Technologies, 2000). The detail of each functions shows follow.

F.1 Resolution Bandwidth

The resolution bandwidth (RBW) determines the analyzer's frequency resolution. It may effect how fast the analyzer makes a measurement. Normally, resolution bandwidth is adjusted automatically as the frequency span is selected. RBW is one of the most important parameter setting in a spectrum analyzer. Because RBW may affect measurement time, manually selecting a narrow RBW can slow down a measurement. On the other hand, selecting a RBW that is too wide may not give adequate frequency resolution and can obscure spectral components that are close together. In vector mode, the minimum resolution bandwidth is a function of frequency span and the number of frequency points, and the maximum resolution bandwidth is a function of frequency span only.

In this study, the RBW is about 10 (9.99750) kHz (adjusted automatically by HP 89410A).

F.2 Frequency Span

The full-span measurement of HP 89410A is from 0 Hz to 10 MHz. Measurements with spans that start at 0 Hz are often called baseband measurements. In the HP 89410A the sample rate is adjusted, based on the span, to achieve the desired information bandwidth.

In this study, the frequency span was set to cover 0 to 1 MHz.

F.3 Display Resolution and Frequency Span

The number of frequency point of HP 89410A can be selected from 51 to 3201 points of display resolution. However, for a given number of frequency points, narrower spans have finer frequency resolution because the same number of frequency points represents a smaller range of frequencies. The display resolution can be calculated by

$$\text{Display resolution} = \text{Frequency span} / \text{Number of frequency points} - 1 \quad (\text{F.1})$$

In this study, the number of frequency points is 401 points and frequency span is 1 MHz (from subsection E.2).

So

$$\text{Display resolution} = 1 \times 10^6 / (401 - 1) = 2.5 \text{ kHz}$$

F.4 Windowing

A window is a time-domain weighting function applied to the input signal. A window is a filter used to compensate for the fact that most signals are not periodic within the input time record. Depending on the window, the HP 89410A attenuates the ends of the

input time record, to prevent leakage caused by transforming signal that are not periodic within the time record.

In this study, the Flattop window is selected because it has good frequency resolution for a fixed resolution bandwidth and high amplitude accuracy. The window bandwidth (WBW) of Flattop is 3.8193596.

F.5 Time Record Length

The time record length (T) is described in term of window bandwidth (WBW) and resolution bandwidth (RBW). The relationship can be written as (Agilent Technologies, 2000)

$$T = \text{WBW} / \text{RBW} \quad (\text{F.2})$$

Maximum Time Record Length

The maximum time record length (T_{\max}) is limited by the number of frequency points,

$$T_{\max} = (\text{FP} - 1) / \text{Frequency span} \quad (\text{F.3})$$

where FP is the number of frequency points.

Minimum Time Record Length

The minimum time record length (T_{\min}) is dependant on the relation bandwidth to span ratio,

$$T_{\min} = \text{WBW} / \text{RBW}_{\max} \quad (\text{F.4})$$

$$\text{RBW}_{\max} = 0.3 \times \text{Frequency span} \quad (\text{F.5})$$

In this study, the time record length (T) is

$$T = 3.8193596 / 10 \times 10^3 = 381.93 \times 10^{-6} \text{ second}$$

The maximum time record length (T_{\max}) is

$$T_{\max} = (401 - 1) / 1 \times 10^6 = 400 \times 10^{-6} \text{ second}$$

The minimum time record length (T_{\min}) is

$$\text{RBW}_{\max} = 0.3 \times (1 \times 10^6) = 300 \text{ kHz}$$

$$T_{\min} = 3.8193596 / 300 \times 10^3 = 12.73 \times 10^{-6} \text{ second}$$

F.6 Time Record Size

The time record size (TP) refers to the number of time points (samples) in a time record. The TP can be defined as (Agilent Technologies, 2000)

$$\text{TP} = \text{SR} \times T \quad (\text{F.6})$$

$$SR = 2.56 \times \text{Frequency span} \quad (\text{F.7})$$

where SR is the sample frequency rate (in baseband mode).
In this study, time record size (TP) is

$$TP = (2.56 \times 10^6) \times (381.93 \times 10^{-6}) = 988 (977.75) \text{ points}$$

The vector measurement mode, amplitude and phase information in frequency and time domain and also time gating, was set in this study. The all parameters can be summarized as shown below.

RBW	=	10 kHz
Frequency span	=	0-1 MHz
Display resolution	=	2.5 kHz
Time record length (T)	=	381.93×10^{-6} second
Maximum time record length (T_{\max})	=	400×10^{-6} second
Minimum time record length (T_{\min})	=	12.73×10^{-6} second
Time record size (TP)	=	988 points

APPENDIX G

Comparison of AE Spectra between Artificial Leakage and Air Jet at External Ball Valve (Flange)

For comparison of AE spectra between artificial leakage and air jet at external ball valve (flange), artificial leaks from the incomplete closure of a ball valve are used to simulate a leak. The AE spectra of internal ball valve leakage are recorded using the same equipment and under the same conditions as those that are used in internal valve calibration (a 25.4 mm ball valve at inlet pressure from 300 to 500 kPa at three valve leakage rates of 100, 130 and 160 ml/sec).

The AE spectra from internal ball valve leakage are shown in figure 5.10 (AE1 sensor) and figure 5.11 (WD sensor).

The air jet calibration results of AE spectra from external ball valve (flange side) are shown in figure G.1 (AE1 sensor) and figure G.2 (WD sensor). The frequency response of the AE1 and WD sensor is about 100 kHz.

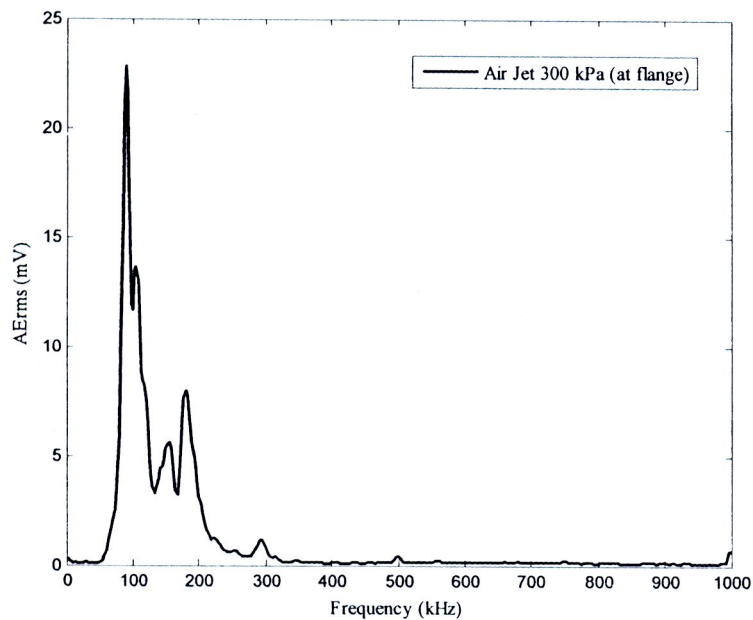


Figure G.1 The AE spectra from external ball valve (flange side) of AE1 sensor

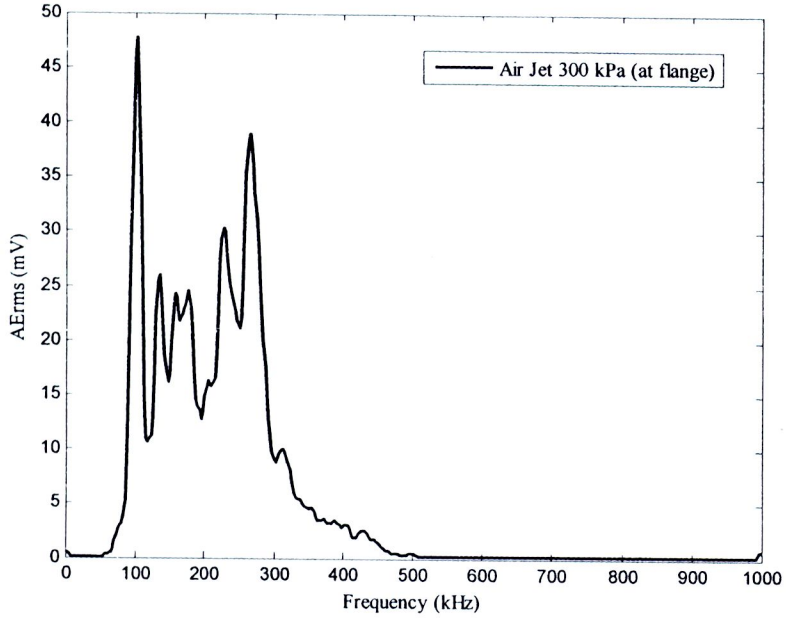


Figure G.2 The AE spectra from external ball valve (flange side) of WD sensor

The average ratios between G_{y1} / G_{y2} (AE1/WD) from both the air jet (flange side) and fluid leakage spectra are shown in figure G.3 and G.4. The ratio of the air jet and the fluid leak between two AE sensors are not similar in shape. This ratio can not use to transfer data between the different AE sensors.

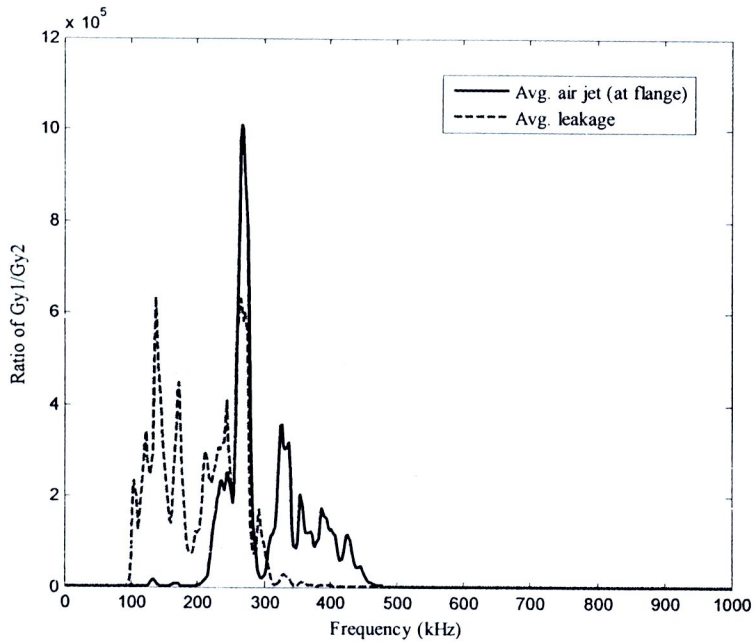


Figure G.3 The average ratio of G_{y1} / G_{y2} (AE1/WD) at flange side for pressure from 300 to 500 kPa and leakage rate from 100-160 ml/sec

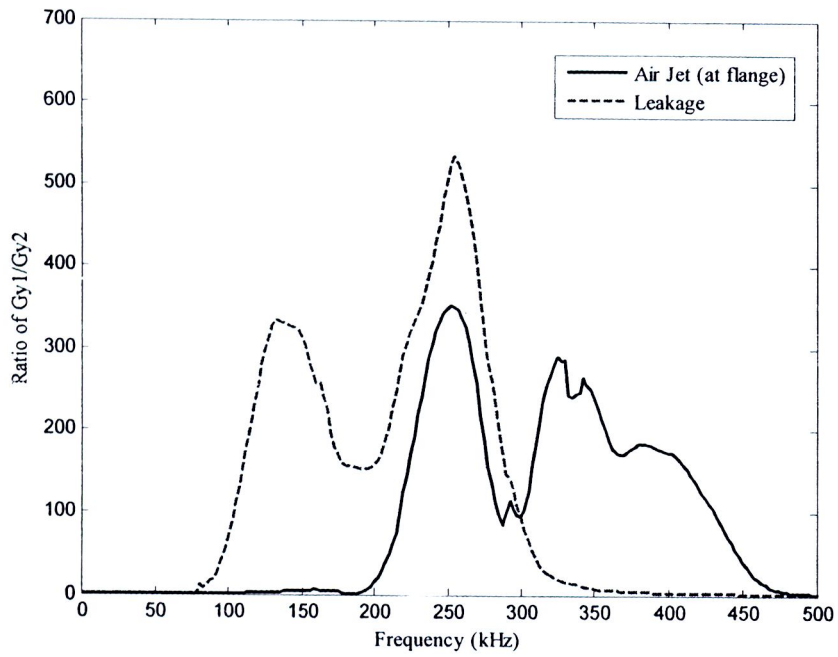


Figure G.4 The average ratio of G_{y1}/G_{y2} (AE1/WD) at flange side

CURRICULUM VITAE

NAME	Mr. Mai Noipitak
DATE OF BIRTH	28 December 1978
EDUCATION RECORD	
VOCATIONAL'S DEGREE	Diploma (Machine Shop Mechanics), Rajamangala Institute of Technology Bangkok Technical Campus, 2002
BACHELOR'S DEGREE	Bachelor of Engineering (Production Engineering), King Mongkut's University of Technology Thonburi, 2005
MASTER'S DEGREE	Master of Engineering (Welding Engineering), King Mongkut's University of Technology Thonburi, 2007
DOCTORAL'S DEGREE	Doctor of Philosophy (Manufacturing and Systems Engineering), King Mongkut's University of Technology Thonburi, 2011
SCHOLARSHIP	Royal Golden Jubilee (RGI) Ph.D. Scholarship, Thailand Research Fund, 2008
	Thailand Graduate Institute of Science and Technology: TGIST, 2006-2007
	King Mongkut's Diamond Scholarships, 2005 - 2006, 2008
PUBLICATIONS	Noipitak, M. and Prateepasen, A., 2011, "Effects of wave propagation paths and system calibration on uniform corrosion monitoring using acoustic emission", CORROSION The Journal of Science and Engineering , Vol. 67, Issue 11, pp.115003-1-115003-10.
	Noipitak, M., Prateepasen, A. and Kaewwaewnoi, W., 2011, "A relative calibration method for a valve leakage rate measurement system", Measurement , Vol. 44, No. 1, pp. 211-218.

Vilasmongkolchai, T., Noipitak M.,
Kaewtrakulpong, P. and Prateepasen, A., 2010,
“Ultrasonic Inspection System for Detecting Small
Flaws at Far Surface of Steel Plate”, **The 2010
International Conference on Electrical
Engineering/Electronics, Computer,
Telecommunications and Information
Technology (ECTI-CON 2010)**, May 19-21,
Chiang Mai, Thailand, pp. 168-172.

Prateepasen, A., Srinang, M. and Noipitak, M.,
2008, “Status of the Thai Society for
Nondestructive Testing and NDT in Thailand”,
**The 17th World Conference on Nondestructive
Testing**, October 25-28, Shanghai, China.

6. If the benefits arise from my thesis or my intellectual property works owned by KMUTT, I shall be entitled to gain the benefits according to the allocation rate stated in the Regulation of King Mongkut's Institute of Technology Thonburi Re the Administration of Benefits deriving from Intellectual Property B.E. 2538.

Signature..... *Mai Noipitak* Transferor
(Mr.Mai Noipitak)
Student

Signature..... *S. Sakamon Devahastin* Transferee
(Assoc. Prof. Dr. Sakamon Devahastin)
Associate Dean for Research and Academic Affairs
(Acting for Dean)

Signature..... *Asa Prateepasen* Witness
(Assoc. Prof. Dr. Asa Prateepasen)

Signature..... *Chaiya Dumkum* Witness
(Asst. Prof. Dr. Chaiya Dumkum)



